ELEMENTAL GEOCHEMISTRY OF THE CRETACEOUS DEPOSIT IN THE DAHOMEY BASIN (NIGERIA): IMPLICATION FOR PALEOCLIMATE AND PALEOENVIROMENTAL RECONSTRUCTION.

***Adesanoye, T.P[1]** and Omietimi, E.J[2]
[1]Department of Geology, University of Ibadan, Ibadan, Nigeria
adesanoyetemitopepaul@gmail.com
[2]Department of Geology, University of Pretoria, South Africa
erepamo.omietimi@tuks.co.za
Journal of African Earth Science –under review

Abstract

In order to determine the ; paleoclimatic, provenance, tectonic setting, Paleo-redox conditions, Paleo-productivity , Paleo-hydrodynamic conditions and paleowater depth of the subsurface samples of Itori well, within the eastern Dahomey basin, compositional studies were carried out on the well from the interval of 55-320m consisting of eighteen (18) limestone and two (2) sandstone samples. These samples were subjected to geochemical analyses entailing major elemental oxides, trace elements as well as rare earths element. The geochemical analysis were conducted using X- ray refraction method (XRF) and inductively Coupled Plasma-Mass Spectroscopy (ICP-MS) respectively. .

The major oxides composition of limestone reveals that; SiO_2, Al_2O_3, Fe_2O_3, TiO_2 and CaO constitute about 90% wt %, oxides such as MgO, Na_2O, K_2O, V_2O_3, ZnO and SrO are < 1wt. % each, while that of sandstone revealed that SiO_2, Al_2O_3, Fe_2O_3, TiO_2 and CaO constituting about 95wt%, oxides such as; MgO, Na_2O, K_2O, V_2O_3, MnO, NiO, ZrO_2, ZnO and SrO are < 1 wt % each. Ti, P and Sr dominated the trace element suites. Sr/Ba ratio indicate a hot, dry climate at the time of deposition with high rate of evaporation indicating a saline environment. The Th/Sc, Th/Co Th/Cr and Cr/Th ratios of the sediments suggested intermediate to felsic provenance. V/Cr, Ni/Co, U/Th and V/(V + Ni) ratio indicate a strongly oxic to dysoxic to anoxic condition. P/Ti ratio indicate high productivity while Zr/Rb ratio indicate deposition of sediments under intermediate to strong paleo-hydrodynamic condition and low- intermediate water depth.

INTRODUCTION.

The geology of the source area, the energy of the transport medium, the increasing distance from the source, freshwater and marine incursions, the depth of the water, the presence or absence of hydrothermal fluids, the climate, weathering, and redox conditions during sedimentation are all significant factors that affect the chemical composition of sedimentary rocks (Moradi et al., 2016). By examining their distinct geochemical signatures, these elements leave their marks on the resulting deposits, which can be interpreted (Pehlivanli, 2019).

The chemical composition of Sedimentary rocks is frequently employed as a sensitive indicator of provenance, lithofacies association, paleo-depositional environment, paleoclimatic conditions, as well as paleo wathering and geochemical maturity of sediment. In certain situations, it is also utilized as a tool to tie together tectonic history (Cullers, 2000). The depositional environment's signature is retained in major elements like Al, Fe, Mn, and Ti, high field strength elements like U, Th, and Zr, large ion lithophile elements like Sr, Ba, and Rb, and transition elements like Co, Zn, Cr, V, Ni, and Cu because they are all transported to the sedimentary basin without significant fractionation (Tribovillard et al., 2006; Kahmann et al., 2008; Moradi et al., 2016). Additionally, the hydrodynamic pressure during sedimentation, the paleoclimate, paleoredox, and hydrothermal conditions can all be evaluated using the immobile chemical elements (Zr, Fe, Al, and Th) and the mobile chemical elements (Sr, Ba, and Rb). Due to their relatively low mobility during sedimentary processes, trace elements like La, Y, Sc, Cr,Th, Zr,Hf,Nb, and especially TiO2, among other major elements, are best suited for provenance and tectonic setting determination (McLennan et al., 1983).

A lot of interest has recently been shown in the eastern Dahomey Basin (Nigeria sector) fig. 1, as new road cut exposures and borehole availability have enhanced our understanding of the region's geology. The extensive occurrences of bitumen, glass sand, and limestone in this basin have made it of great geological interest. In this area of the basin near Okitipupa, east of Lagos, where bituminous sands outcrop, exploration work started in 1908. After oil was discovered in the Niger Delta in 1956, attention was diverted from the eastern Dahomey basin to the Niger Delta, and this exploratory work was later abandoned and termed dry well. Recently, there has been a resurgence of interest in exploration activities in the basin due to increased government incentives to prospectors and re-evaluation of data gathered from previous unsuccessful attempts (Elueze and

Nton, 2004). In order to identify the composition of the sediments, the provenance and paleo-depositional environment, the tectonic history, and the paleo-redox and paleo-productivity of sediments, of the Itori well located in the eastern Dahomey Basin, Southwestern Nigeria this study was embarked upon. These knowledge would be of immense importance to researchers and explorationists.

2. LOCATION OF STUDY AREA AND GEOLOGICAL SETTING

Latitude 7° 6′ 0″ N and longitude 3° 25 ′ 60 ″ define the location of the Itori well in the eastern Dahomey Basin in southwest Nigeria (fig 1). Meanwhile, latitudes $6^0$00N and 7^0 00N and longitudes $2^0$30E and $5^0$00E define the boundaries of the eastern Dahomey Basin in southwest Nigeria (Fig. 2). The Dahomey Basin, which stretches from the Volta Delta in Ghana in the west to the Okitipupa Ridge in Nigeria in the east, is a large sedimentary basin on the Gulf of Guinea's continental margin (Whiteman, 1982) fig(3). The width of the basin is measured from the northern onshore boundary in Benin (Dahomey) to the 3,000-meter bathymetric level, and the distance from the Volta delta to the axis of the Okitipupa Ridge or Ilesha spur is around 440 km and the width of the basin measured from the northern onshore margin in Benin (Dahomey) to the 3,000m bathymetric contour is about 224km (Whiteman, 1982).

Up to the shelf break, the onshore portion of the Dahomey Basin in all four participating countries—Ghana, Togo, Benin, and Nigeria—probably occupies no more than 30,400 square kilometers (Whiteman, 1982) (fig 3).This basin is a marginal pull-apart basin (Kleme, 1975) or marginal sag basin (Kingston et al., 1983). It is also referred to as the Benin basin. As the African and South American lithospheric plates split apart and the continental margin collapsed, it formed during the Mesozoic (Jurassic–Cretaceous) period (Burke et al. 1972; Whiteman, 1982). According to Nton (2001), the striking resemblance of the sedimentary sequences in the coastal basins of Brazil and West Africa illustrates the concept of a common fit.

Faults and other tectonic features connected to the landward extension of the Romanche Fracture zone encircle the basin to the west. The Benin Hinge Line, a significant fault that divides the Okitipupa structure from the Niger delta basin and denotes the continental extension of the Chain Fracture Zone, similarly indicates its eastern boundary (Frauchetau and Le Pichon, 1972; Omatsola and Adegoke, 1981); Fig. 3.

The Okitipupa Ridge (Adegoke, 1969) is an underwater ridge that separates the sediments of the Niger Delta from the Dahomey basin, causing the latter to thin out. Adediran and Adegoke (1987) put out the following four stages of an evolutionary model for the Gulf of Guinea region (fig 4), which includes the Dahomey region: stage 1, which is the intracratonic basin's deposition of thick clastic deposits, primarily young sandstones and freshwater shales. stage 2 is composed of reworked sands and silts intercalated with fluviatile-lacustrine shales that were deposited within the grabens during a period of tectonic activity, erosion, and sedimentation; stage 3 is composed of evaporitic deposits in the southern basin and a paraffin sequence in the northern basin that indicates the start of marine incursion into the basin following the separation of South and North America, and Stage 4 is a marine sediments rich in fauna and flora marking the final stage of the development of the Gulf of Guinea basins.

Several scholars have discussed the stratigraphy of the eastern Dahomey Basin, including Jones and Hockey (1964), Reyment (1965), Fayose (1970), Ogbe (1972), Omatsola and Adegoke (1981), Agagu (1985), Billman (1992), Nton (2001), Elueze and Nton (2004), and Nton et al. (2006). Additionally, multiple classification schemes have been proposed. However, disagreements persist over the nomenclature, age determinations, and classification systems for the many lithological units in this basin (Nton et al, 2009). Starting with the Abeokuta Group, the oldest sedimentary unit unconformably sitting on the underlying basement complex (Table 1) and composed of the three Formations, Ise, Afowo, and Araromi sequentially.Grits and conglomerate make up the base of the Ise Formation, which is covered with loose sands with coarse grains and intermediate kaolinite. A NE palaeo-current system is suggested by the cross-bedding azimuth alignments seen in this formation's sandstone and pebble (Nton, 2001). Based on palynomorphs, Omatsola and Adegoke (1981) suggested that this formation is Neocomian in age (most likely Valanginian–Barbian).

The Afowo Formation, which sits on top of the Ise Formation, is primarily made up of coarse to medium-grained sandstone with varying thick interbedded siltstones, clays, and shales, with the proportion of shale rising towards the top. The lowest portion is made up of a succession of brackish to marginal marine strata interspersed with clean, loose, well-sorted, subrounded, and fluviatile sands. Its maximum thickness, as determined by Omatsola and Adegoke in 1981, is 2,300 meters. The Araromi Formation, which was composed of fine to medium-grained sands at the base

and shale and siltstone with thin interbedded limestones and marls on top, lies on top of the Afowo Formation. According to Matsola and Adegoke (1981), this deposit is the youngest of the Cretaceous sequences in the eastern Dahomey basin.

The Ewekoro Formation overlies the Araromi Formation and it is predominately limestone; the top is highly scoured and consists of red, dense, glauconitic, phosphatic and fossiliferous limestone. It is Palaeocene in age and associated with shallow marine environment due to abundance of coralline algae, gastropods, pelecypods, echinoid fragment and other skeletal debris (Nton, 2001).

On top of the Ewekoro Formation is the shaley unit of the Akinbo Formation (Ogbe, 1972), consisting of dark micro micaceous, fine-textured shale that is locally silty with glauconitic marl and conglomerate at the base (Dessauvagie, 1975). It consists of laminated and glauconitic shale and kaolinitic clay sequence (Nton and Elueze, 2005. The Oshosun Formation, which is composed of sandstone interbeds and greenish-grey or beige clay and shale, sits atop the Akinbo Formation. The shale is glauconitic and heavily laminated. Phosphate is present in this deposit, which has phosphorite composition (Nton, 2001). In the eastern Dahomey basin, the Ilaro Formation sits atop the Oshosun Formation and is composed of large, poorly cemented, yellow, cross-bedded sandstone (Nton, 2001). The Benin Formation, which is the youngest sedimentary unit in the eastern Dahomey basin, is made up of a number of sands that have been poorly sorted, some of which include cross-bedded areas, and clay lenses (Agagu, 1985).

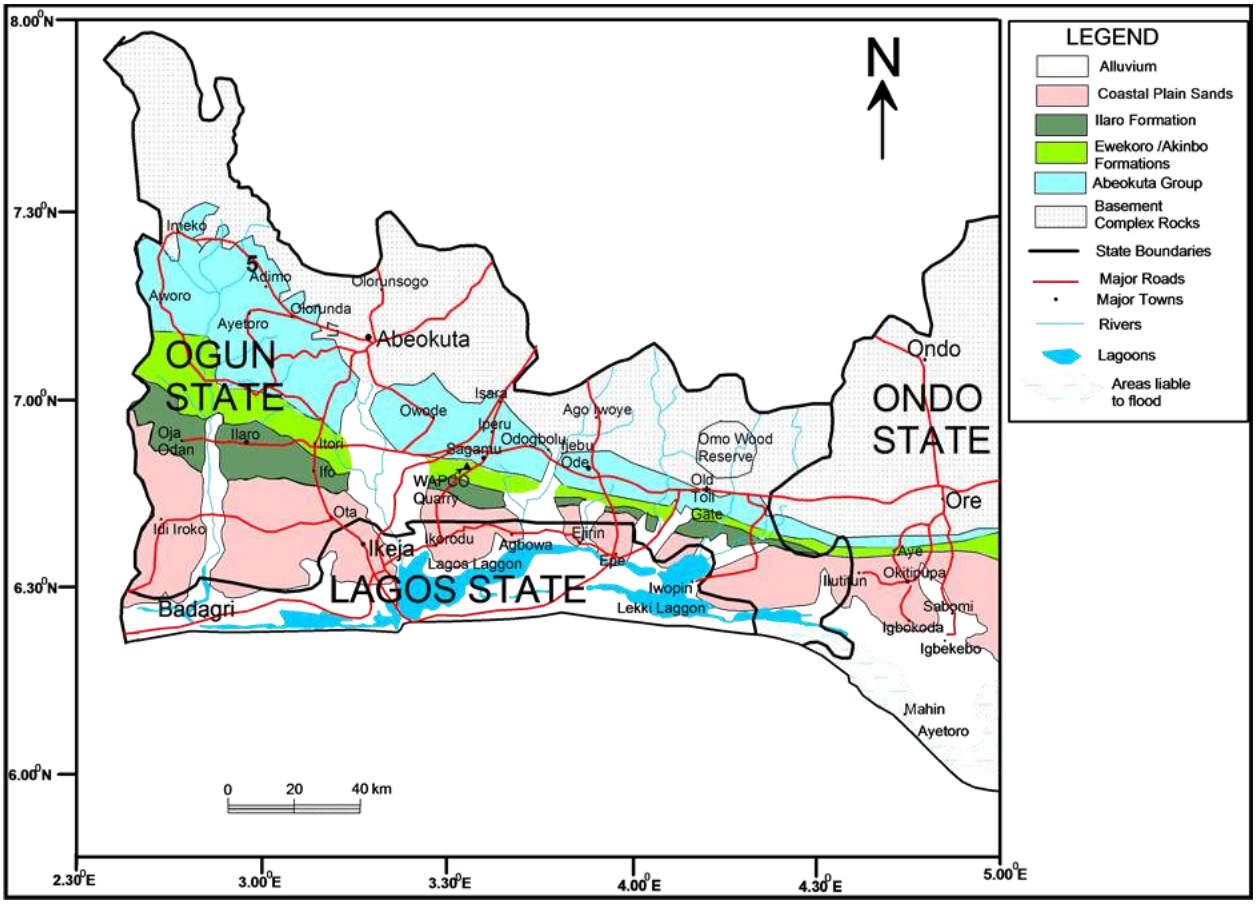

Fig 1. Geological map of Dahomey Basin in the Nigerian sector and the states located on the basin (modified after Jones, H.A. and Hockey, R.D. (1964)

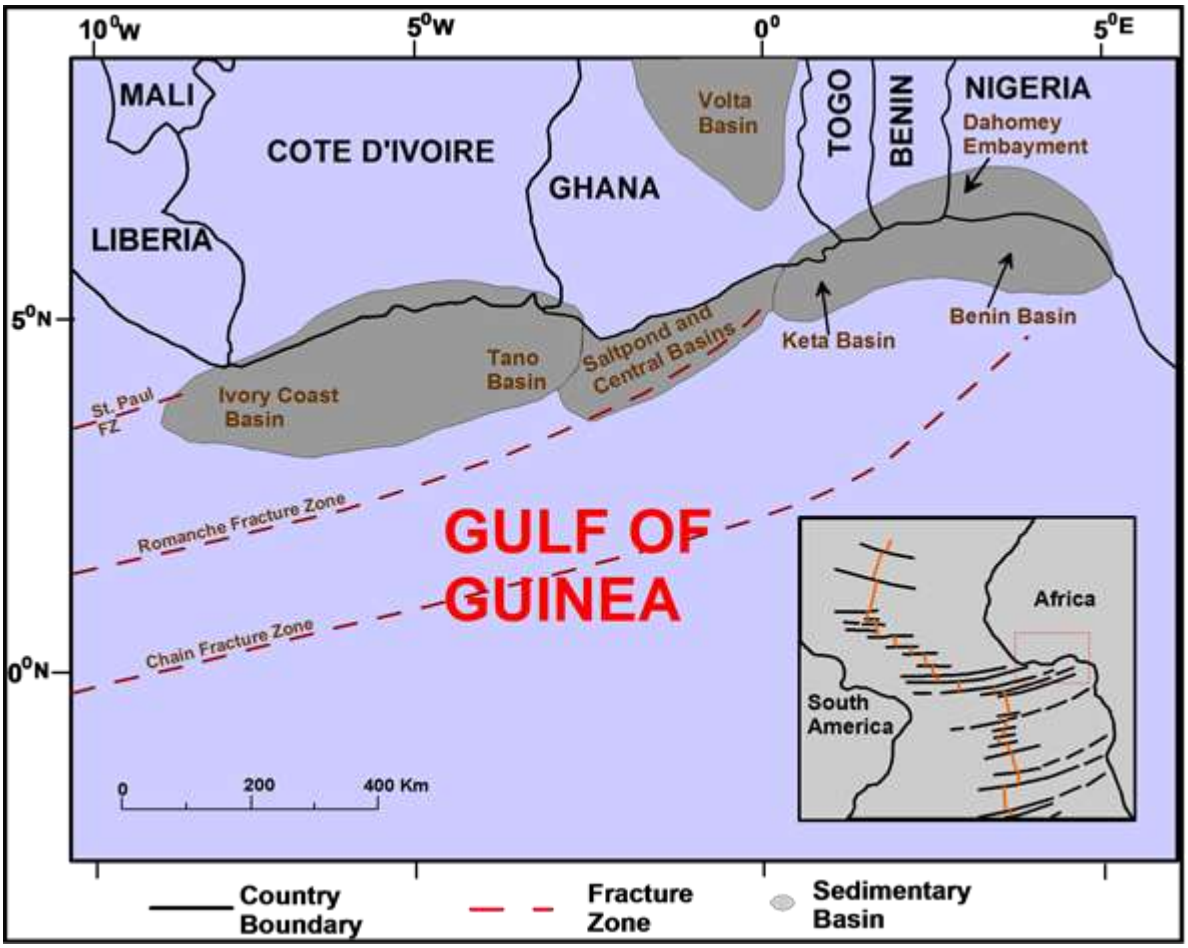

Fig 2. Regional map of the Gulf of Guinea showing the location of Benin (Dahomey) Basin in relation to other basins (modified after Brownfield, M.E. and Charpentier, R.R. (2006).

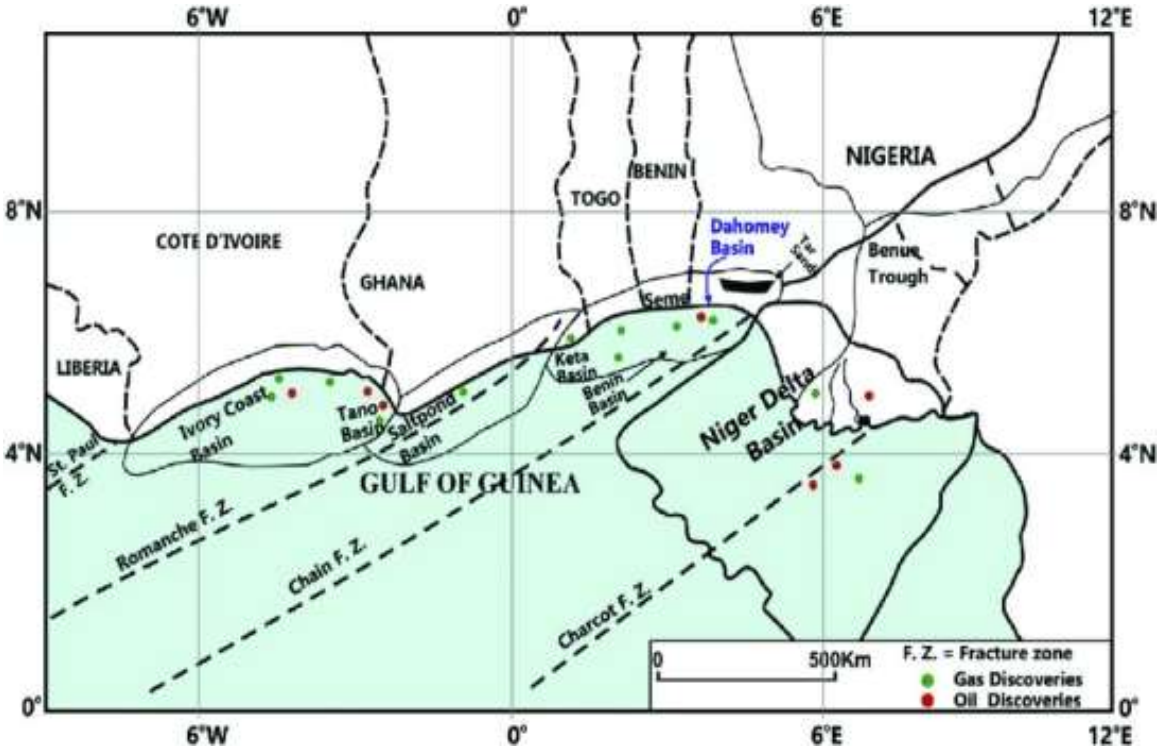

Fig 3: Major features of the Gulf of Guinea Province, West Africa: Dahomey, Keta, Saltpond, Tano, and Ivory Coast basin from the east to the west (After Brownfield and Chapentier, 2006.)

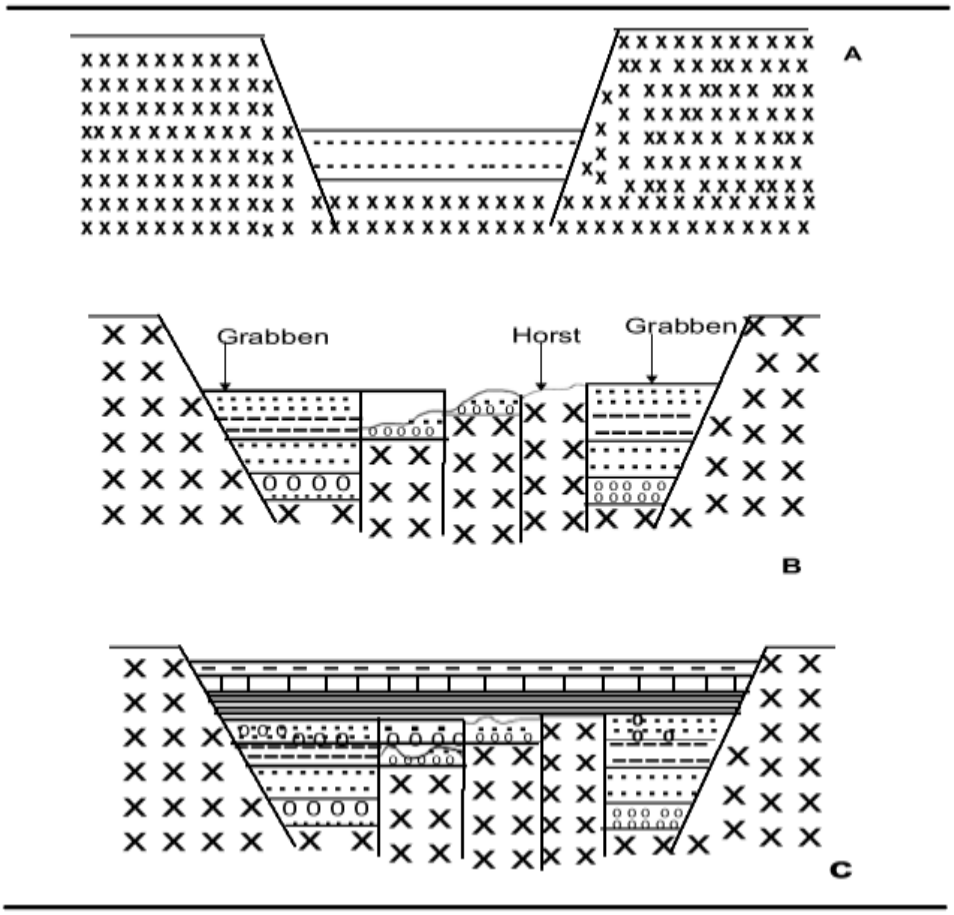

Fig 4: Tectonic model of the evolution of Dahomey basin. After, (Omotsola and Adegoke, 1981) A) Subsidence of the basement before the South American rift. B) Santonian folding of the Dahomey Basin sediments, the folding resulted in faulting and rifting resulting in the formation of horst and graben. C) Post Separation deposition of subsequent invading sediment.

Table 1: Generalized stratigraphic column showing age, lithology, and sequence of the formations and tectonic stage of basin development in the Nigerian sector of the Benin Basin.

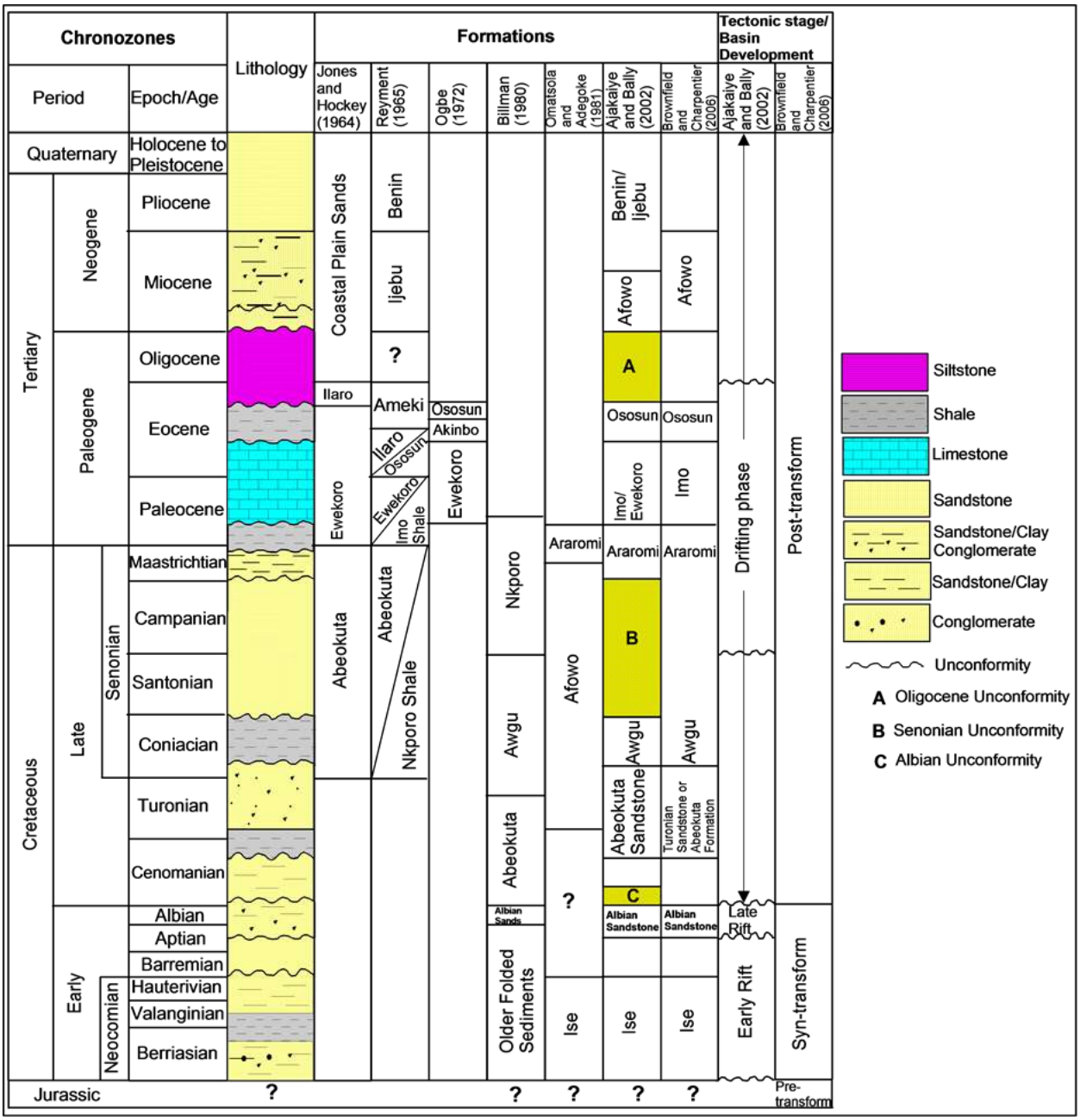

3. SAMPLES AND METHODS

For this study, subsurface samples of Itori well, located within the eastern Dahomey basin, were obtained from the Nigeria Geological Survey Agency (NGSA), Kaduna. These samples were logged and taken in well –labeled sample bags to the Department of Geology, University of Ibadan for further examination and selection for laboratory analyses. A total of twenty (20) representative sample from depth ranging from 55m to 320m consisting of eighteen (18) limestone and two (2) sandstone samples were selected for subsequent analyses. Twelve (12) samples were selected for geochemical analysis. The samples were first pulverized and about 2-3 grams of each was weighed out using a sensitive electrical digital weighing balance for analyses. Each pulverized samples was taken into a sample cup and analyzed for their major oxides. The samples were dried and roasted in alumina refractory crucibles, @ 100°C and 1000°C respectively, to determine Loss on Ignition (LOI). 1g of each sample was mixed with 6g Lithiumeteraborate flux and fused at 1030°C to make a stable fused glass bead. The Thermo Fisher ARL Perform'X Sequential XRF instrument with Uniquant software, was used for the analysis. The software analyzed for all elements in the periodic table between Na and U, but only elements found above the detection limits were reported. The values were normalized, to include LOI, to determine crystal water and oxidation state changes. A standard sample material was prepared and analyzed in the same manner as the samples and reported as such. The XRF analysis was carried out at Stoneman's Laboratory, Department of Geology, University of Pretoria, South Africa. Twenty (12) samples were used for minor and REE geochemical analysis (electronic supplementary material 1). Circa 7–10 g of each sample, pulverized to <75 μm in a Tungsten Carbide milling vessel, was roasted at 1000 ^{o}C to determine Loss on ignition (LOI), and fused into a glass bead. Aliquot of the sample was pressed into a powder briquette to determine trace elements. Preparation of samples and analyses were carried out using standard methods after Loubser and Verryn (2008).Analyses of trace elements and REE were conducted at the Earth Lab, of the University of Witwatersrand, South Africa, using a Thermo Scientific iCAPRQ for inductively coupled plasma mass spectrometry (ICP-MS)

4 RESULTS

4.1 BULK GEOCHEMISTRY

4.1.1 Major oxide geochemistry

The elemental oxides for the sandstone have the following ranges; SiO_2 (33.29 -71.83wt %), Al_2O_3 (2.03- 3.97wt %), Fe_2O_3 (1.95-2.40wt %), TiO_2 (0.17 - 0.18wt %) and CaO (11.8 - 31.0wt %) Table 2. Other oxides such as MgO, Na_2O, K_2O, V_2O_3, MnO, NiO, ZrO_2, ZnO, SrO are less than 1 percent (< 1wt %) each. limestone has the following composition; SiO_2 (13.03 - 53.23wt %), Al_2O_3 (0.22 - 2.56wt %), Fe_2O_3 (0.6 - 12.87wt %), TiO_2 (0.02-0.12wt %) and CaO (12.95 - 46.6wt %). Other oxides such as MgO, Na_2O, K_2O, V_2O_3, MnO, NiO, ZrO_2, ZnO, SrO are less than 1 percent (< 1wt. %) each. The SiO_2 values for the sandstone indicate low compositional maturity and low to high degree of weathering (Pettijohn, 1963). The concentration of Al_2O_3, and Fe_2O_3 in the rock types is a clear indication of weathering processes (Tijani *et al.*, 2010). The low value of TiO_2 content in the samples suggest more felsic material in the source rocks (Taylor and McLennan, 1985). The high values of CaO in both rock types are associated with the limestone of the Ewekoro Formation in the basin.

4.1.2 Trace element geochemistry.

The result of the trace element concentration show that Ti dominates the trace element suites with value ranging from 373.40 - 944.33ppm (av., 1027ppm). Others are; P (293.83 - 557.88ppm; av., 576.54ppm); Sr (126.04 - 543.88 ppm; av. 304.54 ppm) Table 3. The value of Sr is lower than the average values for lithospheric carbonate where Sr= 610 ppm (Turekian and Wedepohl, 1961). Ranges of other trace elements are as follows; Zr (4.65 - 426.17ppm, av 52.05ppm), Cr (10.82 - 141.73, av 43.0ppm), Zn (15.42 - 268.01, av 79.0ppm), V (5.04 - 258.34ppm, av. 79.0ppm); Th (0.43-11.32ppm, av 2.09ppm) and Ba (5.20 - 36.94, av 6.0ppm). The abundance of high field strength elements such as; Cr and Zr, can be related to the presence of detrital minerals such as chrome spinel and zircon (Hunstsman- Mapilaa *et al.*, 2005). Strontium (Sr) and Barium (Ba) are two elements with different geochemical behaviors. According to Liu (1980), the Sr/Ba ratio is regarded as an indicator of paleo- salinity

4.1.3 Rare element geochemistry

The range of Total ΣREE contents (1.199-226.83 ppm; average = 44.26 ppm; n =12) showed significant variations among the samples Table 4. The ΣREE contents are higher than the range for marine carbonates; 0.04-14 ppm (Turekian and Wedepohl, 1961) and average typical marine carbonates ~ 28 ppm (Bellanca *et al*., 1997).

Table 2: Distribution of major oxide concentration (%) in the study well

	IT2	IT5	IT13	IT14	IT16	IT17	IT19	IT22	IT26	IT28	IT 30	IT 32	AVG
Oxides	Sandstones		Limestone										
SiO_2	71.83	33.29	39.18	53.32	51.76	41.35	23.64	43.27	42.65	29.87	22.9	13.03	38.84
Al_2O_3	2.03	3.97	2.56	1.47	0.29	0.22	0.95	0.23	0.49	0.33	0.74	0.31	1.13
MgO	0.36	0.64	1.22	1.49	0.62	0.61	1.62	0.87	1.55	0.55	0.54	0.42	0.87
Na_2O	<0.01	<0.01	<0.01	<0.01	<0.01	<0.01	<0.01	<0.01	<0.01	<0.01	<0.01	<0.01	<0.01
P_2O_5	0.18	0.15	0.23	0.34	0.07	0.08	0.25	0.06	0.07	0.06	0.21	0.14	0.15
Fe_2O_3	1.95	2.4	7.58	12.87	0.58	0.6	1.56	0.74	0.82	0.64	1.06	0.6	2.62
K_2O	0.13	0.18	0.16	0.1	0.01	0.01	0.07	0.01	0.02	0.01	0.02	0.01	0.06
CaO	11.48	31	24.31	12.95	24.94	30.16	38.41	29.19	28.3	37.31	40.42	46.6	29.59
TiO_2	0.18	0.17	0.77	0.26	0.12	0.05	0.06	0.03	0.06	0.02	0.03	0.02	0.15
V_2O_5	<0.01	<0.01	0.04	0.01	<0.01	<0.01	<0.01	<0.01	<0.01	<0.01	<0.01	<0.01	0.03
Cr_2O_3	0.01	<0.01	0.03	0.01	<0.01	<0.01	<0.01	<0.01	<0.01	<0.01	<0.01	<0.01	0.02
MnO	0.05	0.09	0.08	0.09	0.03	0.03	0.04	0.02	0.02	0.04	0.07	0.05	0.05
NiO	<0,01	<0,01	0.01	<0.01	<0.01	<0,01	<0.01	<0.01	<0.01	<0.01	<0.01	<0.01	0.01
CuO	<0.01	<0.01	<0.01	<0.01	<0.01	<0.01	<0.01	<0.01	<0.01	<0.01	<0.01	<0.01	<0.01
ZrO_2	0.13	0.07	0.74	0.15	0.1	0.05	0.03	0.05	0.06	0.03	0.02	0.02	0.12
S	0.52	0.53	0.23	0.04	<0.01	<0.01	0.03	0.23	0.06	0.01	0.01	0.01	0.17
C_3O_4	<0.01	<0.01	<0.01	0.01	<0.01	<0.01	<0.01	<0.01	<0.01	<0.01	<0.01	<0,01	0.01
ZnO	0.01	0.01	0.04	0.01	<0.01	0.01	<0.01	<0.01	<0.01	<0.01	<0.01	<0.01	0.02
SrO	0.06	0.13	0.07	0.04	0.06	0.08	0.15	0.09	0.1	0.09	0.13	0.12	0.09
WO_3	<0,01	0.01	0.01	<0.01	<0.01	<0.01	<0.01	<0.01	<0.01	<0.01	<0.01	<0.01	0.01
LOI	11.09	27.35	22.75	16.81	21.4	26.7	33.18	25.15	25.77	31.01	33.82	38.64	26.14

Table 3: Distribution of trace element concentration (ppm) in the-study well

ppm	IT2	IT5	IT13	IT14	IT16	IT17C	IT19	IT22	IT26	IT28	IT30	IT32	Total	AVG
	Sandstones		Limestone											
Sc	2.86	5.79	11.81	5.66	0.76	0.70	2.29	0.65	0.95	0.86	2.13	1.29	35.75	2.97
Co	4.83	3.62	9.64	5.17	0.35	0.39	1.91	1.01	0.94	0.71	2.55	1.34	32.46	2.70
Cu	4.13	6.19	5.54	4.18	2.79	3.89	3.17	3.11	3.72	4.49	4.22	5.22	50.64	4.22
Ni	12.10	12.03	20.14	11.50	2.33	2.29	5.38	4.46	4.29	3.73	8.35	4.65	91.25	7.60
V	15.50	21.33	258.34	121.3	5.04	5.23	18.66	5.53	9.08	8.28	22.48	10.70	501.45	41.78
Zn	46.77	49.09	268.01	60.78	19.36	46.99	30.36	15.42	31.40	26.47	52.60	21.31	668.55	55.8
Cr	23.87	31.82	141.73	52.48	14.52	13.47	25.73	10.82	33.97	17.12	32.52	27.17	425.21	43.0
Zr	27.51	22.09	426.17	86.22	9.76	9.18	11.26	4.65	9.29	6.17	7.67	4.70	624.67	52.05
Cs	0.34	0.70	0.31	0.21	0.07	0.07	0.23	0.08	0.15	0.10	0.18	0.10	2.53	21.0
Hf	0.84	0.55	10.64	2.45	0.28	0.24	0.32	0.13	0.24	0.17	0.22	0.13	16.20	35 .0
Nb	2.17	3.22	7.31	3.11	1.07	1.54	1.12	0.62	1.08	0.58	0.79	0.64	23.24	94 .O
Rb	5.26	10.36	6.26	3.62	1.33	1.31	4.61	1.76	3.03	2.23	3.21	1.74	44.73	73 .0
Sr	141.9	389.38	213.78	126.4	155.63	257.88	543.14	282.95	304.31	330.50	449.03	460.24	3654.83	304.6
Th	1.60	1.92	11.32	3.71	0.59	0.43	1.06	0.49	0.92	0.65	1.57	0.88	25.12	2.09
U	1.06	1.17	2.46	0.87	0.36	0.35	1.96	0.63	0.49	0.32	0.98	0.45	11.11	0.93
Ba	24.95	27.92	36.94	36.91	6.42	5.20	12.14	6.04	8.15	9.50	10.77	7.11	192.03	16.00
Pb	4.76	4.04	17.74	7.39	2.30	1.30	1.62	2.07	2.44	1.59	4.43	2.51	52.19	4.35
P	549.9	550.88	551.88	552.9	553.88	554.88	555.88	556.88	557.88	293.83	977.39	662.32	6918.48	576.5
Li	22.17	53.33	19.18	10.02	3.54	3.01	10.42	2.90	5.74	2.98	6.28	2.89	142.45	11.87
Sb	0.36	0.14	0.43	0.32	0.09	0.08	0.07	0.19	0.14	0.11	0.21	0.10	2.25	0.19
Ta	0.15	0.19	0.46	0.23	0.06	0.23	0.07	0.03	0.06	0.04	0.05	0.05	1.61	0.13
W	0.48	0.30	0.67	0.31	0.43	1.05	0.13	0.11	0.19	0.47	0.70	0.90	5.73	0.48
Tl	0.03	0.03	0.02	0.01	-0.00	-0.00	0.00	0.00	-	0.00	0.01	0.00	0.10	0.01
AS	5.14	0.94	3.20	1.84	0.14	0.15	0.50	0.62	0.42	1.60	1.07	0.55	16.16	1.35
Ga	3.23	5.26	5.92	3.26	0.85	0.65	2.60	0.82	1.52	1.12	3.00	1.55	29.78	2.48
Ti	944.3	127.34	436.14	1427	849.02	373.40	777.41	495.30	697.04	448.06	457.89	476.25	11307	1027
P/Ti	0.58	0.43	0.013	0.39	0.66	1.49	0.715	1.12	0.8	0.66	2.14	1.39	10.39	0.87
U/Th	0.66	0.61	0.22	0.24	0.61	0.81	1.85	1.29	0.53	0.49	0.62	0.51	8.44	0.70
V/Cr	0.65	0.67	1.822	2.31	0.35	0.39	0.73	0.51	0.27	0.48	0.69	0.37	9.24	0.77
Ni/co	2.51	3.31	2.04	2.23	6.66	5.87	2.81	4.41	4.56	5.25	3.27	3.47	46.39	3.87
Sr/Ba	5.69	13.95	5.79	3.41	24.24	49.59	44.74	46.85	37.34	34.79	41.69	64.73	372.81	31.07

Cu/Zn	0.09	0.13	0.02	0.07	0.14	0.08	0.07	0.20	0.12	0.17	0.08	0.24	1.41	0.12
Zr/Rb	5.23	0.21	68.08	23.81	7.33	7.43	2.44	2.64	3.07	2.77	2.39	2.70	128.10	10.68
Th/Cr	0.07	0.06	0.08	0.07	0.04	0.03	0.06	0.05	0.03	0.04	0.05	0.03	0.61	0.05
Cr/Th	14.29	16.67	12.50	14.29	25.00	33.30	16.67	20.00	33.30	25.00	20.00	33.30	264.32	22.03
Th/Sr	0.56	0.33	0.96	0.66	0.78	0.61	0.46	0.75	0.97	0.76	0.73	0.68	8.25	0.69
Th/Co	0.33	0.53	1.17	0.71	0.89	1.10	0.55	0.49	0.98	0.92	0.62	0.66	8.95	0.75
V/(V/ Ni)	0.56	0.64	0.93	0.91	0.68	0.70	0.78	0.55	0.68	0.70	0.73	0.70	8.56	0.71
Sr/Cu	34.37	62.90	38.59	30.15	55.78	66.29	171.34	90.98	97.85	73.61	106.41	88.17	916.44	76.37
Th/Sc	0.56	0.33	0.96	0.66	0.78	0.61	0.46	0.75	0.97	0.76	0.74	0.68	8.22	0.69
Th/U	1.51	1.64	4.60	4.26	1.64	1.23	0.54	0.78	1.88	2.03	1.60	1.96	23.67	1.97
Rb/Sr	0.04	0.03	0.03	0.03	0.009	0.005	0.08	0.06	0.01	0.007	0.007	0.004	0.31	0.03
Zr/Rb	5.23	2.13	68.30	23.82	7.34	6.9	2.44	2.64	2.82	2.77	2.39	2.70	129.48	10.79

Table 4: Distribution of rare element concentration (ppm) for the study well

Ppm	IT2	IT5	IT13	IT14	IT16	IT17C	IT19	IT22	IT26	IT28	IT30	IT32	∑REE	AVG
	Sandstones		Limestone											
La	10.325	15.26	19.52	12.604	4.06	3.107	10.472	4.303	6.837	5.807	18.162	8.029	118.486	9.87
Ce	20.093	27.198	48.302	31.116	6.351	4.829	21.936	6.591	11.188	8.289	28.409	12.54	226.839	8.90
Pr	2.218	2.95	4.979	3.242	0.88	0.695	2.486	0.948	1.625	1.34	3.984	1.827	27.174	2.26
Nd	8.812	11.182	20	13.013	3.67	2.856	10.397	3.976	6.808	5.603	16.264	7.669	110.25	9.19
Sm	1.669	1.891	4.344	2.57	0.715	0.595	1.915	0.807	1.285	1.095	3.087	1.497	21.47	1.79
Eu	0.378	0.42	1.053	0.619	0.171	0.143	0.445	0.192	0.297	0.256	0.704	0.342	5.02	0.42
Gd	1.522	1.575	4.116	2.315	0.694	0.596	1.726	0.779	1.163	1.028	2.727	1.37	19.611	1.63
Tb	0.205	0.207	0.629	0.326	0.098	0.083	0.224	0.109	0.153	0.141	0.375	0.185	2.735	0.23
Dy	1.168	1.19	3.783	1.903	0.577	0.505	1.25	0.639	0.875	0.825	2.143	1.053	15.911	1.33
Y	6.151	6.939	20.267	9.11	3.58	3.486	7.985	4.436	5.55	5.802	13.751	7.708	94.765	7.90
Ho	0.224	0.228	0.747	0.36	0.115	0.099	0.228	0.127	0.169	0.16	0.403	0.212	3.072	0.26
Er	0.615	0.615	2.154	0.977	0.312	0.268	0.586	0.341	0.446	0.427	1.058	0.547	8.346	0.70
Tm	0.089	0.088	0.342	0.149	0.045	0.038	0.078	0.047	0.059	0.059	0.145	0.075	1.214	0.10
Yb	0.57	0.566	2.373	0.96	0.281	0.232	0.49	0.281	0.366	0.344	0.86	0.454	7.777	0.65
Lu	0.086	0.087	0.377	0.145	0.043	0.035	0.074	0.043	0.055	0.052	0.131	0.071	1.199	0.10

5. DISCUSSION

5.1. Implications of Ca/Mg and Mg/Ca Ratios for Palaeo-Salinity.

The petrogenetic classification of carbonate rocks using the standard ratio Ca/Mg and reciprocal ratio Mg/Ca was presented by Todd, T.W. in 1966 Table 5. The following are the class limits of the standard ratio of Ca/Mg > 100 - 39.0, 39.0 - 12.3, 12.3 - 5.67, 5.67 - 1.86, 1.86 - 1.50, 1.50 - 1.22, and 1.22 - 1.00, representing limestone, magnesian limestone, dolomitic limestone, dolomitized limestone, calcareous dolomite, dolomite, and magnesian dolomite, respectively: Additionally, the following class limits of the reciprocal ratio, Mg/Ca, of 0 - 0.03, 0.03 - 0.08, 0.08 - 0.18, 0.18 - 0.54, 0.54 - 0.67, 0.67 - 0.82, and 0.82 - 1.00 are expressed as limestone, magnesian limestone, dolomitic limestone, dolomitized limestone, calcareous dolomite, dolomite, and magnesian dolomite, respectively.

The standard and reciprocal ratios of Ca and Mg composition of the Ewekoro limestone are shown in table below. 60% of the samples are classified as “magnesian limestone, 30% as pure limestone and 10% as dolomitic limestone.

The Ca/Mg ratio has implications for the stability conditions of the depositional environment that led to the formation of the carbonate(s). Naturally, the Mg/Ca ratio increases during evaporation of sea water, especially under saline environmental conditions. Considering the Ca/Mg and Mg/Ca ratios, it can be concluded that the relative rate of evaporation of sea water and the palaeo-salinity condition was low, as such limestone (30%) was deposited more at the expense of dolomite (10%). However, intermittent increase in rate of sea water evaporation and salinity resulted to the deposition of the magnesian limestones (60%). The low – intermittent rate of evaporation is characteristic of a warm and humid climate at the time of deposition of sediment.

5.2. Provenance.

According to Bhatia and Crook, 1986; McLennan and Taylor, 1991; Cullers, 2000, many HSFEs (e.g., Th, Zr, and Hf) and TTEs (e.g., Cr,Co, and Sc) in sedimentary rocks can provide important clue for their sedimentary provenance. Ratios such as La/Th, La/Sc, Cr/Th, Co/Th, and Sc/Th are widely used as provenance indicators (Jian et al., 2013; Ma et al., 2015; Moradi et al., 2016; Chatterjee et al., 2022), also, sedimentary rocks of felsic origins are generally associated with low La/Th, Co/Th, and Cr/Th ratios (Condie and Wronkiewicz, 1990; Floyd and Leveridge, 1987; Amorosi et al., 2002; Cullers, 2002).

The Co/Th, Cr/Th, Sc/Th, and La/Sc ratios of the studied samples in the Itori well is 0.59–3.02 (avg 1.48), 14.15 –36.92 (avg. 22.94), 1.03–3.02 (avg. 1.58), and 1.72-11.57 (avg. 7.45).

Some elemental ratios such as; Th/Sc, Th/Co and Th/Cr, Cr/Th, show significant variations in felsic and mafic rocks and are widely used to investigate the source area composition (Wronkiewicz and Condie, 1990; Cox *et al*., 1995; Cullers, 1995; Armstrong-Altrin *et al*., 2004; Armstrong-Altrin,2009)

5.3. Tectonic setting

Previous conventional identification diagrams of SiO_2–K_2O/Na_2O (Roser and Korsch, 1986), have long been used to distinguish the tectonic setting of passive continental margins, active continental margins, and continental and oceanic island arcs. However, the above conventional diagrams are rarely successful in tectonic setting identification, as re-evaluated by Armstrong-Altrin and Verma (2005), and they should be used with more caution. Recently, Verma and Armstrong-Altrin (2013, 2016) proposed two new multidimensional discriminant function diagrams for the tectonic setting discrimination of low-silica [(SiO2)adj = 35–63%] and high-silica [(SiO2)adj = 63–95%] clastic rocks based on the log ratio values of major oxides. The subscript ‘‘adj” represents the normalization to 100% of major elements, excluding the LOI. More details are presented in Verma and Armstrong-Altrin (2013, 2016). These two multidimensional diagrams can effectively distinguish island arc, collision, and rift settings, and they have recently become widely used (Moradi et al., 2016; Deng et al., 2019). To accurately reveal the tectonic setting of rocks during their deposition,we used these two multidimensional diagrams instead of the previous traditional identification diagrams. The SiO_2 for the sandstone is 33.29 -71.83wt %, and for the limestone is

SiO_2 13.03 - 53.23wt % avg (38.84). Both the low- and high-silica indicate a sediment deposited in content dominantly in the Active Continental Margin and Passive Continental Margin, suggesting a syn-rift faulting setting of a transform margin. It also suggested that the sediments comes from multiple sources, of igneous and metamorphic basement rocks plus reworked older clastic sediments

5.4 Paleo-redox conditions and Paleo-productivity.

Because they become immobile after deposition and burial, elements like V, U, Fe, Mn, Co, Cr, and Ni are referred to as redox sensitive elements and they show the redox properties of the depositional environment (Jones and Manning, 1994). According to Goldberg and Humayun (2016), redox sensitive components are therefore excellent and trustworthy proxies for determining the paleo-redox conditions of sedimentary rocks. The present investigation employed reference standards for U/Th, V/Cr, Ni/Co, and V/(V + Ni) to characterize the paleo-redox conditions. According to Li et al. (2018), V/Cr ratios > 4.25 typically indicate an anoxic depositional environment, or strong reducing conditions; ratios between 2.0 and 4.25, on the other hand, indicate a dysoxic depositional setting, or reducing conditions; and ratios <2.0, an oxic depositional environment, or oxidizing conditions. According to Jones and Manning (1994) and Guo et al. (2011), Ni/Co levels >7.0 imply an anoxic depositional environment, 5.0–7.0 indicate a dysoxic environment, and <5.0 suggests oxic conditions. Jones and Manning (1994) stated that U/Th ratios >1.25 suggest anoxic circumstances, 0.75–1.25 reflect dysoxic situations, and <0.75 show oxic conditions. Last but not least, according to Hatch and Leventhal (1992), V/(V + Ni) ratios >0.84 suggest euxinic depositional conditions, or anaerobic-reducing conditions; 0.54–0.82 implies anoxic settings; and 0.46–0.60 indicates dysoxic depositional situations. V/Cr from the well under study ranges from 0.27 to 2.31 (av. 0.77 ppm), showing oxic sediment deposition. Ni/Co levels vary from 2.04-5.87 ppm (av. 3.87), which is likewise indicative of oxic conditions. A dysoxic environment is indicated by a U/Th value of 0.22–0.62 ppm (avg 0.77 pm), Furthermore, Table 4 shows that the V/(V + Ni) ratio ranges from 0.55 to 0.93 ppm (av. 0.71 ppm), suggesting anoxic deposition. We can conclude that the sediments from the Itori well were deposited in conditions ranging from strongly oxic to dysoxic to anoxic condition (Nton and Adeyemi, 2014). According to Hallberg (1976), in a sedimentary environment, high Cu/Zn ratios suggest reducing

depositional circumstances, while low Cu/Zn values indicate oxidizing depositional conditions. The Cu/Zn ratio in the examined well is between 0.02 to 0.24, which suggests an oxidizing environment.

The amount of organic matter that organisms may produce per unit space and time during the energy cycle is known as paleo-productivity (Chen et al., 2021a). The variations in primary productivity have been inferred from the abundance of certain specific geochemical indicators, such as Ba, P, Cu, Ni, and Zn (Schenau et al., 2005; Schoepfer et al., 2015). For instance, trace element ratios of P/Ti offer important insights into nutritional conditions and paleo-productivity, which is the uptake of dissolved inorganic carbon and its sequestration into organic compounds by primary marine producers (Tribovillard et al., 2006; Li et al., 2020; Zhang et al., 2020). Phosphorus is important for all kinds of life on earth since it is a major component of skeletal material and is involved in a variety of metabolic activities (Li *et al*., 2020; Zhang *et al.*, 2021). Li *et al*., (2020) provided the following thresholds; P/Ti value < 0.34 lower; 0.34–0.79 intermediate, and P/Ti >0.79 indicates high productivity (Li *et al*., 2020). In this study, the P/Ti ratio ranges from 0.013-2.14ppm (average 0.87ppm) Table 3, indicating high productivity.

5.5 Paleo-hydrodynamic conditions and paleowater depth.

According to Pehlivanli (2019), this explains the energy state of the water mass during the deposition of old sedimentary rocks. As said by Pehlivanli in 2019. While Rb is a common mobile element in a wide range of geological processes and accumulates in deep water with low energy due to its active chemical features, Zr is a common element that is preserved in continental, transitional, and shallow-marine habitats (Li et al., 2018b). The Zr/Rb ratio is thought to be a reliable predictor of paleo-hydrodynamic conditions because it can respond to variations in water depth (Teng, 2004; Teng et al., 2005; Zhao et al., 2016; Li et al., 2018b; Pehlivanli, 2019). The hydrodynamic pressure is less and the water depth is greater when the Zr/Rb ratio is smaller.In this study, the Zr/Rb ratio ranged from 0.21 - 68.08 (av., 10.97 ppm) Table 3, indicating deposition of sediments under intermediate to strong paleo-hydrodynamic condition and low- intermediate water depth. (Teng, 2004; Pehlivanli, 2019).

Table 5: Range of elemental ratios in this study compared to the ratios in sediments derived from felsic rocks, mafic rocks, Upper Continental Crust (UCC) and Post-Archean Australian shale (PAAS).

Elemental ratio	Range for present study[1] Min	Max	Range of sediment[2] Felsic rock	Maficrock	UCC[3]	PAAS[3]	Remark on provenance
Th/Sc	0.3	0.97	04.0-0.94	0.71-0.95	0.63	0.66	Intermediate-felsic rock
Th/Co	0.33	0.89	0.67-19.40	0.04-1.40	0.63	0.63	Intermediate-felsic rock
Th/Cr	0.03	0.08	0.13-2.70	0.02-0.05	0.13	0.13	Intermediate-felsic rock
Cr/Th	12.50	33.30	4.00-15.00	25-500	7.76	7.53	Intermediate-felsic rock

[1]Present study, n = 12, [2](Cullers 1994, 2000; Cullers and Podkovyrov, 2000; Cullers et al. (1988); [3]Taylor and McLennan, 1985)

TABLE 6: petrogenetic classification of carbonate rocks using the standard ratio Ca/Mg and reciprocal ratio Mg/Ca was presented by Todd, T.W. in 1966.

sample no	CaO(wt%)	MgO(wt%)	Standard ratio Ca/Mg	Reciprocal ratio Mg/Ca	Descriptive terms
IT 13	24.31	1.22	19.9	0.05	magnesian limestone
IT 14	12.95	1.49	8.7	0.115	dolomite limestone
IT 16	24.94	0.62	40.2	0.024	magnesian limestone
IT 17	30.16	0.61	49.4	0.020	magnesian limestone
IT19	38.41	1.62	23.7	0.042	magnesian limestone
IT22	29.19	0.87	33.6	0.029	magnesian limestone
IT26	28.3	1.55	18.2	0.055	magnesian limestone
IT28	37.31	0.55	67.8	0.015	Limeston
IT 30	40.42	0.54	74.9	0.013	Limestone
IT 32	46.6	0.42	100	0.009	Limestone

CONCLUSION

The major oxides composition of limestone reveals that; SiO_2, Al_2O_3, Fe_2O_3, TiO_2 and CaO constitute about 90% wt %, oxides such as MgO, Na_2O, K_2O, V_2O_3, ZnO and SrO are < 1wt. % each, while that of sandstone revealed that SiO_2, Al_2O_3, Fe_2O_3, TiO_2 and CaO constituting about 95wt%, oxides such as; MgO, Na_2O, K_2O, V_2O_3, MnO, NiO, ZrO_2, ZnO and SrO are < 1 wt % each. Ti, P and Sr dominated the trace element suites. Sr/Ba ratio indicate a hot, dry climate at the time of deposition with high rate of evaporation indicating a saline environment, modal sandstone composition consists of sub rounded quartz grain, monocrystalline and polycrystalline quartz grains, rock fragment, rutile, garnet and tourmaline, suggest a mixed provenance of metamorphic, plutonic and recycled sedimentary sources. The Th/Sc, Th/Co Th/Cr and Cr/Th ratios of the sediments suggested intermediate to felsic provenance. V/Cr, Ni/Co, U/Th and V/(V + Ni) ratio indicate a strongly oxic to dysoxic to anoxic condition. P/Ti ratio indicate high productivity while Zr/Rb ratio indicate deposition of sediments under intermediate to strong paleo-hydrodynamic condition and low- intermediate water depth. It can be deduced that the sandstone is a product of recycled nearby basement rock while the limestone is of shallow marine origin with terrigenous influx.

REFERENCES

Adediran, S.A and Adegoke, O.S., (1991). The continental sediment of the Nigerian coastal basins. Journal of Africa Earth science. 12(1/2), 79-84.

Adegoke ,O.S., Ako, B.D., and Enu, E.I. (1980). Geotechnical investigations of the Ondo State bituminous sands. Vol. 1. Geology and reserve estimate. Rept. Geological Consulting Unit, Dept. of Geology, University of Ife. 257pp

Adegoke, O.S. (1969); Eocene Stratigraphy of Southern Nigeria. Bulletining Bureau de Research Geologic ET Miners Memoir, 69, 23-48.

Agagu, O.A. (1985): A Geological Guide to Bituminous Sediments in South Western Nigeria. Unpublished Report, Department of Geology, University of Ibadan, Ibadan.

Akaegbobi and Ogungbesan (2016): Geochemistry of the Paleocene Limestones of Ewekoro Formation. Ife Journal of Science vol. 18, no. 3.

Akpo, B.D (1980): Stratigraphy of Oshosun Formation in Southwestern Nigeria. Journal of Mining and Geology Vol .1(1):77-106.

Algeo, T.J., and Tribovillard, N. (2009): Environmental analysis of paleoceanographic systems based on molybdenum-uranium covariation. Chem. Geol. 268, 211–225.

Armstrong-Altrin, J.S., Lee, Y.I., Verma, S.P., and Ramasamy, S. (2004): Geochemistry of sandstones from the Upper Miocene Kudankulam Formation Southern India:implications for provenance, weathering and tectonic setting. J. Sediment. Res.74, 285–297.

Armstrong-Altrin, J.S., Verma, S.P., Madhavaraju, J., Lee, Y.I., and Ramasamy, S. (2003): Geochemistry of Late Miocene Kudankulam Limestones, South India International Geology Review, 45, 16–26.

Bhatia, M.R. (1983). Plate tectonics and geochemical composition of sandstones: Journal of Geology. 91, 611-627

Bechtel, A., Jia, J.L., Strobl, S.A.I., Sachsenhofer, R.F., Liu, Z., Gratzer, R. and Püttmann, W., (2012): Paleoenvironmental conditions during deposition of the Upper Cretaceous oil shale sequences in the Songliao Basin (NE China): implications from geochemical analyses. Org. Geochem. 46, 76–95.

Bellanca, A., Claps, M., Erba, E., Masetti, D., Neri, R., Premoli-Silva, I., and Venezia, (1996), Orbitally induced limestone/marlstone rhythms in the Albian-Cenomanian Cismon section (Venetian region, northern Italy): Sedimentology, calcareous and siliceous plankton distribution, elemental and isotope geochemistry. Palaeogeography, Palaeoclimatology, Palaeoecology, v. 126, p.14 227–260.

Berggren, W. A., (1960). Paleocene Biostratigraphy and Planktonic Foraminifera of Nigeria (West Africa), Proc. 21st Inter. Geol. Cong. Copenhagen, 6, 41-55.

Billman, H.G., (1992): Offshore Stratigraphy and Paleontology of the Dahomey Embayment, West Africa. Nigerian Association Petroleum Explorationists Bulletin, 7, 121-130.

Brownfield, M.E. and Charpentier, R.R., (2006): Geology and Total Petroleum Systems of the Gulf of Guinea Province of West Africa: U.S Geological Survey Bulletin 2207-C, 32p.

Chen, L., Jiang, S., Chen, P., Chen, X., Zhang, B., Zhang, G., Lin, W., Lu, Y., (2021). Relative sea-level changes and organic matter enrichment in the Upper Ordovician-Lower Silurian Wufeng-Longmaxi Formations in the Central Yangtze area, China.Mar. Pet. Geol. 124, 104809.

Chen, Q., Li, Z., Dong, S., Yu, Q., Zhang, C., Yu, X., (2021): Applicability of chemical weathering indices of eolian sands from the deserts in northern China. CATENA 198,105032.

Cheng, Y., Liu, W., Wu, W., Zhang, Y., Tang, G., Liu, C., Nie, Q., Wen, Y., Lu, P. and Zhang, C., (2021): Geochemical characteristics of the lower Cambrian Qiongzhusi Formation in Huize area, east Yunnan: implications for paleo-ocean environment and the origin of black rock series. Arab. J. Geosci. 14, 1–16.

Chivas, A.R., Deckker, P. and Shelley, J.M.G., (1986): Strontium content of Ostracoda indicates paleosalinity. Nature 316, 251–253.

Cox, R., Low, D.R., and Cullers, R.L. (1995): The influence of sediment recycling and basement composition on evolution of mudrock chemistry in the southwestern United States. Geochimica et Cosmochimica Acta, 59, 2919–2940.

Culler R.L., (2000): The geochemical of shales, siltstone and Sandstone vof Pennsylvania-Permian age, Colorado, USA: Implications for provenance and metamorphic studies. Chemical Geology. 51,181-203.

Cullers, R.L. (1994): The controls on the major and trace element variation of shales, siltstones and sandstones of Pennsylvanian – Permian age from uplifted continental blocks in Colorado to platform sediment in Kansas, USA: Geochimica et Cosmochimica Acta, 58(22), 4955-4972.

Cullers, R.L. (1995): The controls on the major and trace element evolution of shales, siltstones and sandstones of Ordovician to Tertiary age in the Wet Mountain region, Colorado, U.S.A. Chemical Geology, 123, 107–131.

Cullers, R.L. (2000): The geochemistry of shales, siltstones and sandstones of Pennsylvanian-Permian age, Colorado, U.S.A.: implications for provenance and metamorphic studies: Lithos, 51, 305-327.

Cullers, R.L. and Podkovyrov, V.N. (2000): Geochemistry of the Mesoproterozoic Lakhanda shales in southeastern Yakutia,Russia: implications for mineralogical and provenance control, and recycling. NO JOURNAL

Cullers, R.L., Basu, A. and Suttner, L. (1988): Geochemical signature of provenance in sand-size material in soils and stream sediments near the Tobacco Root batholith, Montana, USA: Chemical Geology, 70(4), 335- 348.

Deng, H.W., Qian, K., (1993): Sedimentary Geochemistry and Environment Analysis. GansuTechnology Publishing House, Lanzhou, pp. 1–150.

Dickinson, W. R. (1970). Interpreting detrital model of greywacke and arkose. Journal of Sedimentary Petrology, 40, 695 – 707

Elueze, A. A. and Nton, M. E. (2004): Organic geochemical appraisal of limestones and shales in part of eastern Dahomey Basin, southwestern Nigeria. Journal of Mining and Geology, Vol.40 No.1, 29-40

Fayose, E. A. and Asseez, L. O., (1972): Micropaleontological investigation of Ewekoro area, southwestern Nigeria. Micropaleontology, 18, (3), 369 – 385.

Fayose, E.A. (1970): Stratigraphic paleontology of Afowo-1 well, SW Nigeria. J. Min. Geol. Nig. 5(1), 23-34.

Fayose, E.A. and Azeez, L.O. **(1972)**; Micropalaeontological Investigations of Ewekoro Area, Southwestern Nigeria. Micropaleontology, 18, 369-385.http://dx.doi.org/10.2307/1485014.

Fedo, C.M., Wayne Nesbitt, H., and Young, G.M., (1995): Unraveling the effects of potassium metasomatism in sedimentary rocks and paleosols, with implications for paleoweathering conditions and provenance. Geology 23, 921–924.

Goldberg, K. and Humayun, M., (2016): Geochemical paleoredox indicators in organic-rich shales of the Irati Formation, Permian of the Parana Basin, southern Brazil. Brazilian J. Geol. 46, 377–393.

Goldberg, K., and Humayun, M., (2016): Geochemical paleoredox indicators in organic-rich shales of the Irati Formation, Permian of the Parana Basin, southern Brazil. Brazilian J. Geol. 46, 377–393.

Hallberg, R.O., (1976): A geochemical method for investigation of palaeoredox conditions in sediments. Ambio Special Rep. 4, 139–147.

Hatch, J.R., and Leventhal, J.S., (1992): Relationship between inferred redox potential of the depositional environment and geochemistry of the Upper Pennsylvanian (Missourian) Stark Shale Member of the Dennis Limestone, Wabaunsee County, Kansas, USA. Chem. Geol. 99, 65–82.

Huang, H., He, D., Li, D., Li, Y., Zhang, W., Chen, J., (2020). Geochemical characteristics of organic-rich shale, Upper Yangtze Basin: implications for the Late Ordovician–Early Silurian orogeny in South China. Palaeogeogr. Palaeoclimatol. Palaeoecol. 554, 109822.

Jones, B. and Manning, D.A.C., (1994): Comparison of geochemical indices used for the interpretation of palaeoredox conditions in ancient mudstones. Chem. Geol. 111, 111–129.

Jones, H.A. and Hockey, R.D. (1964): The Geology of Part of Southwestern Nigeria. Geological Survey of Nigeria Bulletin, 31, 1-101.

Kahmann, J.A., Seaman, J. and Driese, S.G., (2008): Evaluating trace elements as paleoclimate indicators: multivariate statistical analysis of late Mississippian Pennington Formation paleosols, Kentucky, USA. J. Geol. 116, 254–268.

Li, D., Li, R., Zhu, Z., Wu, X., Liu, F., Zhao, B., Cheng, J., Wang, B., (2018). : Elemental characteristics and paleoenvironment reconstruction: a case study of the Triassic lacustrine Zhangjiatan oil shale, southern Ordos Basin, China. Acta Geochim. 37, 134–150.

Li, D., Li, R., Zhu, Z., Xu, F., (2018): Elemental characteristics of lacustrine oil shale and its controlling factors of palaeo-sedimentary environment on oil yield: a case from Chang 7 oil layer of Triassic Yanchang Formation in southern Ordos Basin. ActaGeochim. 37, 228–243.

Li, H., Liu, B., Liu, X., Meng, L., Cheng, L. and Wang, H., (2019): Mineralogy and inorganic geochemistry of the Es4 shales of the Damintun Sag, northeast of the Bohai Bay Basin: implication for depositional environment. Mar. Pet. Geol. 110, 886–900.

Li, T.-J., Huang, Z.-L., Chen, X., Li, X.-N. and Liu, J.-T., (2021): Paleoenvironment and organic matter enrichment of the Carboniferous volcanic-related source rocks in the Malang Sag, Santanghu Basin, NW China. Pet. Sci. 18, 29–53.

Li, X., Gang, W., Yao, J., Gao, G., Wang, C., Li, J., Liu, Y., Guo, Y. and Yang, S., (2020): Major and trace elements as indicators for organic matter enrichment of marine carbonate rocks: A case study of Ordovician subsalt marine formations in the central-eastern Ordos Basin, North China. Mar. Pet. Geol. 111, 461–475.

Long, X., Yuan, C., Sun, M., Xiao, W., Wang, Y., Cai, K., Jiang, Y., (2012). Geochemistry and Nd isotopic composition of the Early Paleozoic flysch sequence in the Chinese Altai, Central Asia: evidence for a northward-derived mafic source and insight into Nd model ages in accretionary orogen. Gondwana Res. 22, 554–566.

McLennan, S.M., Taylor, S.R., McCulloch, M.T. and Maynard, J.B., (1990): Geochemical and Nd-Sr Isotopic Composition of Deep Sea Turbidites: Crustal Evolution and plate Tectonic Association. Geochemical et Cosmochimica Acts, 54, 2015-2050.

McLennan, S.M., Hemming, S., McDaniel, D.K., Hanson, G.N. 1993. Geochemical approaches to sedimentation , provenance, and tectonics. In: Johnson, M.J., Basu, A. (eds.), Processes Controlling the Composition of Clastic Sediments: Geological Society of America, Special Paper 284, 21-40

Moradi, A.V., Sarı, A. and Akkaya, P., (2016): Geochemistry of the Miocene oil shale (Hançili Formation) in the Çankırı-Çorum Basin, Central Turkey: Implications for Paleoclimate conditions, source–area weathering, provenance and tectonic setting Sediment. Geol. 341, 289–303.

Nton, M.E and Otoba, O.W., (2011). Lithofacies and Organic Geochemical studies of Akinside 1582 well, Eastern Dahomey Basin, Southwestern Nigeria. Nigerian Association of Petroleum Explorationist Bulletin, Vol. No. 23, No. 1, 107-117.

Nton, M.E. and Adeyemi, M.O., (2014): Petrography, compositional characteristic and stable isotope geochemistry of the Ewekoro Formation from Ibese Corehole, eastern Dahomey Basin, southwestern Nigeria. Global Journal of Geological Sciences Vol. 13, pg. 35-52

Nton, M.E. **Ezeh, F.P. and Elueze, A.A. (2006):** Aspects of source rock evaluation and diagenetic history of the Akinbo Shale, eastern Dahomey Basin, southwestern Nigeria. Nigerian Association of Petroleum Explorationists Bulletin, Vol. 19, No. 1, 35-48,

Obaje, N. G. (2009): Geology and Mineral Resources of Nigeria (221 p). Berlin: Springer.https://doi.org/10.1007/978-3-540-92685-6

Ogbe, F.G.A. (1972): Stratigraphy of Strata Exposed in Ewekoro Quarry, Western Nigeria. In: Dessauvagie, T.F.J. and Whiteman, A.J., Eds., African Geology, University of Ibadan Press, Ibadan, 305-322.

Okosun, E.A. (1990): A review of the Cretaceous stratigraphy of the Dahomey Embayment, West Africa. Cretaceous Res 11(1): 17-27

Okosun, E.A. (1998) Review of the Early Tertiary Stratigraphy of Southwestern Nigeria. Journal of Miming and Geology, 34, 27-35.

Olabode, S.O. (2006): Siliciclastic Slope Deposits from the Cretaceous Abeokuta Group, Dahomey (Benin) Basin, Southwestern Nigeria. Journal of African Earth Sciences, 46, 187-200.http://dx.doi.org/10.1016/j.jafrearsci.2006.04.008

Omatsola, M.E., Adegoke, O.S., (1981): Tectonic evolution and Cretaceous stratigraphy of the Dahomey basin. J. Min. Geol. 8, 30–137.

Onuoha, K.M. and Ofoegbu, C.O., (1988). Subsidence and evolution of Nigeria's continental margin: implications of data from Afowo-1 well. Mar. Petrol. Geol. 5, 175–181.

De Matos, D. and Renato, M., (2000): Tectonic evolution of the equatorial South Atlantic. In: Atlantic Rifts and Continental Margins. American Geophysical Union. Geophys. Monogr. Ser., v. 115, p. 331 - 354.

Overare, B., Osokpor, J., Ekeh, P.C. and Azmy, K., (2020). Demystifying provenance signatures and paleo-depositional environment of mudrocks in parts of south-eastern Nigeria: Constraints from geochemistry. J. Afr. Earth Sci. 172, 103954.del ages in accretionary orogen. Gondwana Res. 22, 554–566.

Pehlivanli, B.Y., (2019): Factors controlling the paleo-sedimentary conditions of Çeltek oil shale, Sorgun-Yozgat/Turkey. Maden Tetkik ve Arama Dergisi 158, 251–263.

Reyment R (1965): Aspects of the Geology of Nigeria, University of Ibadan Press, p 144

Rimmer, S.M., (2004): Geochemical paleoredox indicators in Devonian–Mississippian black shales, Central Appalachian Basin (USA). Chem. Geolo. Geochem. Organic-Rich Shales: New Perspect. 206, 373–391. https://doi.org/10.1016/j.chemgeo.2003.12.029.

Roser, B.P. and Korsch, R.J. (1986). Determination of tectonic setting of sandstone mudstone suites using SiO_2 content and K_2O/Na_2O ratio. Jour. Geol. 94, 635–650

Schenau, S.J., Reichart, G.J. and De Lange, G.J., (2005): Phosphorus burial as a function of paleoproductivity. Geochim. Cosmochim. Acta 69, 919–931.

Schoepfer, S.D., Shen, J., Wei, H., Tyson, R.V., Ingall, E. and Algeo, T.J., (2015): Total organic carbon, organic phosphorus, and biogenic barium fluxes as proxies for paleomarine productivity. Earth Sci. Rev. 149, 23–52.

Slanky, M., (1962): Contribution a a'etude geologique du basin sedimentaire cotier au Dahomey at du Togo: Bureau du Recherches geologiques of Minieres, Memoir 11, 270p.

Song, Y., Li, S. and Hu, S., (2019): Warm–humid paleoclimate control of salinized lacustrine organic–rich shale deposition in the Oligocene Hetaoyuan Formation of the Biyang Depression, East China. Int. J. Coal Geol. 202, 69–84.

Tao, S., Xu, Y., Tang, D., Xu, H., Li, S., Chen, S., Liu, W., Cui, Y. and Gou, M., (2017): Geochemistry of the Shitoumei oil shale in the Santanghu Basin, Northwest China:Implications for paleoclimate conditions, weathering, provenance and tectonic setting. Int. J. Coal Geol. 184, 42–56.

Taylor, S.R. and McLennan, S.M. (1985): The continental crust: its composition and evolution. Blackwell, London, p 312.

Teng, G.E., (2004): The distribution of elements, carbon and oxygen isotopes on marine strata and environmental correlation between them and hydrocarbon source rocks formation - An example from Ordovician Basin, China. PhD Dissertation. Graduate School of Chinese Academy of Sciences (Lanzhou Institute of Geology), Lanzhou (in Chinese)

Teng, G.E., Liu, W.H., Xu, Y.C. and Chen, J.F., (2005): Correlative study on parameters of inorganic geochemistry and hydrocarbon source rocks formative environment. Adv.Earth Science 20, 193–200.

Tribovillard, N., Algeo, T.J., Lyons, T. and Riboulleau, A., (2006): Trace metals as paleoredox and paleoproductivity proxies: an update. Chem. Geol. 232, 12–32.

Turekian, K.K. and Wedepohl, K.H. (1961): Distribution of elements in some major units of earth's crust. Geological Society of America Bulletin, 72, 175–192.

Wei, W. and Algeo, T.J., (2020): Elemental proxies for paleosalinity analysis of ancient shales and mudrocks. Geochim. Cosmochim. Acta 287, 341–366.

Wei, Y., Li, Xiaoyan, Zhang, R., Li, Xiaodong, Lu, S., Qiu, Y., Jiang, T., Gao, Y., Zhao, T. and Song, Z., (2021): Influence of a paleosedimentary environment on shale oil enrichment: a case study on the Shahejie Formation of Raoyang Sag, Bohai Bay Basin, China. Front. Earth Sci. 9, 736054 https://doi.org/10.3389/feart.2021.736054.

Whiteman, A. J. (1982): Nigeria Its petroleum geology, resources and potentials. (1) 176, (2) 238.Graham and Trotman, London, U.K.

Wronkiewicz, D.J. and Condie, K.C., (1990): Geochemistry and mineralogy of sediments from the Ventersdorp and Transvaal Supergroups, South Africa: Cratonic evolution during the early Proterozoic Geochimica et Cosmochimica Acta, 54, 343–354.

Xu, J., Liu, Z., Bechtel, A., Meng, Q., Sun, P., Jia, J., Cheng, L. and Song, Y., (2015): Basin evolution and oil shale deposition during Upper Cretaceous in the Songliao basin (NE China): implications from sequence stratigraphy and geochemistry. Int. J. Coal Geol. 149, 9–23.

Xu, Z., Lu, H., Zhao, C., Wang, X., Su, Z., Wang, Z., Liu, H., Wang, L. and Lu, Q., (2011): Composition, origin and weathering process of surface sediment in Kumtagh Desert, Northwest China. J. Geogr. Sci. 21, 1062–1076.

You, J., Liu, Y., Zhou, D., Zheng, Q., Vasichenko, K., and Chen, Z., (2020): Activity of hydrothermal fluid at the bottom of a lake and its influence on the development of high-quality source rocks: Triassic Yanchang Formation, southern Ordos Basin, China. Aust. J. Earth Sci. 67, 115–128.

Zhang, K., Liu, R., Liu, Z., Li, L., Wu, X. and Zhao, K., 2020): Influence of palaeoclimate and hydrothermal activity on organic matter accumulation in lacustrine black shales from the Lower Cretaceous Bayingebi Formation of the Yin'e Basin, China. Palaeogeogr. Palaeoclimatol. Palaeoecol. 560, 110007 https://doi.org/10.1016/j. palaeo.2020.11 0007.

Zhang, L., Dong, D., Qiu, Z., Wu, C., Zhang, Q., Wang, Y., Liu, D., Deng, Z., Zhou, S., Pan, S., (2021): Sedimentology and geochemistry of Carboniferous-Permian marine- continental transitional shales in the eastern Ordos Basin, North China. Palaeogeogr. Palaeoclimatol. Palaeoecol. 571, 110389.

Zhang, L., Xiao, D., Lu, Shuangfang, Jiang, S., Lu, Shudong, (2019): Effect of sedimentary environment on the formation of organic-rich marine shale: Insights from major/trace elements and shale composition. Int. J. Coal Geol. 204, 34–50.

Zhao, B.S., Li, R.X., Wang, X.Z., Wu, X.Y., Wang, N., Qin, X.L., Cheng, J.H. and Li, J.J., (2016): Sedimentary environment and preservation conditions of organic matter analysis of Shanxi formation mud shale in Yanchang exporation area, Ordos Basin. Geol. Sci.Technol. Inform. 35, 109–117.

Zheng, R. and Liu, H., (1999): Study on palaeosalinity of Chang-6 oil reservoir set in Ordos Basin. Oil Gas Geol. 20, 20–25.

Zhong, D.K., Jiang, Z.K., Guo, Q. and Sun, H.T., (2015): A review about research history, situation and prospects of hydrothermal sedimentation. J. Palaeogeogr. 17,285–296

.